



## Development of Ultra-High Temperature Ceramic Matrix Composites for Hypersonic Applications via Reactive Melt Infiltration and Mechanical Testing under High Temperature

*L. Baier<sup>1\*</sup>, Dr. M. Friess<sup>1</sup>, N. Hensch<sup>1</sup>, Dr. V. Leisner<sup>2</sup>*

*<sup>1</sup>German Aerospace Center (DLR), Institute of Structures and Design,  
Pfaffenwaldring 38-40, 70569 Stuttgart, Germany*

*<sup>2</sup>German Aerospace Center (DLR), Institute of Materials Research,  
Linder Höhe, 51147 Cologne, Germany*

### Abstract

In the ongoing development of hypersonic technologies, material advancements play a key role in meeting the ever-increasing thermomechanical demands of these applications. Ultra-High Temperature Ceramic Matrix Composites (UHTCMCs) offer a promising solution for components operating under such extreme conditions. Their outstanding thermomechanical properties, including high temperature and thermal shock resistance, excellent thermal conductivity and mechanical strength, position them as ideal candidates for applications in fields like leading edges or inlet ramps for ramjets and scramjets. Due to their remarkable material composition, UHTCMCs are capable of operating in temperature regimes that surpass 1700 °C during their operation times under oxidizing atmospheres. At the German Aerospace Center (DLR), a UHTCMC material based on carbon fibres and a zirconium diboride matrix is being developed utilizing Reactive Melt Infiltration (RMI). With RMI, the orientation of the reinforcement fibres can be tailored, to enable the material to fulfill the demanding load requirements. The reactive melt infiltration process comprises three stages: preform fabrication, pyrolysis, and the actual melt infiltration. The foundation for important material properties of the final ceramic, including the matrix composition, is established in the preform production, which is a crucial step in the process. A boron- and zirconium diboride-based slurry is infiltrated into pitched-based carbon fibre fabric. Subsequently, the preforms are consolidated, pyrolysed, and infiltrated with molten  $Zr_2Cu$  to obtain the UHTC matrix by in situ reaction with the preform elements. Scanning Electron Microscopy (SEM) and Energy-dispersive X-Ray Spectroscopy (EDX) enable examination of the microstructural features, including the arrangement and distribution of zirconium diboride within the matrix. Mechanical evaluation of the UHTCMCs is conducted via 3-point bending tests at both room temperature and at elevated temperature at 900 °C. It has been demonstrated that Ultra-High Temperature Ceramic Matrix Composites can be produced by means of reactive melt infiltration, and that they retain their strength even at elevated temperatures.

**Keywords:** *Ultra-High Temperature Ceramic Matrix Composite, Ceramic Matrix Composite, Ultra-High Temperature Ceramics, Reactive Melt Infiltration, Mechanical Testing*

### Nomenclature

B – Boron	C/HfB <sub>2</sub> – Carbon fibre reinforced hafnium diboride
C – Carbon	C/ZrB <sub>2</sub> – Carbon fibre reinforced zirconium diboride
C/C – Carbon Carbon	
C/SiC – Carbon fibre reinforced silicon carbide	

CMC – Ceramic Matrix Composite	UHTC – Ultra-High Temperature Ceramic
Cu – Copper	UHTCMC – Ultra-High Temperature Ceramic Matrix Composite
DLR – German Aerospace Center	Zr – zirconium
EDX – energy dispersive X-ray spectroscopy	ZrB <sub>2</sub> – zirconium diboride
HfB <sub>2</sub> – hafnium diboride	ZrC – zirconium carbide
RMI – reactive melt infiltration	F – fibre
SEM – Scanning electron microscope	M – matrix
SiC/SiC – silicon carbide fibre reinforced silicon carbide	

## 1. Introduction

The applications of hypersonic technology in the speed range above Mach 5 has recently been a steadily growing field in the aerospace industry, especially in the areas of re-entry vehicles and cruise missiles [1]. The requirements are defined by trajectories at low altitudes and thus in an oxidative atmosphere with flight times of less than one hour. In addition, these vehicles aim to be maneuverable. For aerodynamic reasons, sharp-edged geometries with small nose radii are preferred for these hypersonic vehicles, as they offer higher Lift-over-Drag ratios which improves maneuverability. These geometries in turn lead to extremely high heat loads occurring at the edges, as the heat flow increases inversely proportional to the nose radius and can reach a value of several  $10^2 \text{ MW/mm}^2$ , which can lead to temperatures in excess of  $2000 \text{ }^\circ\text{C}$  [2–4]. For this reason, in the ongoing development of hypersonic technologies, material advancements play a key role in meeting the ever-increasing thermomechanical demands of these applications. For years, Ceramic Matrix Composite (CMC) materials have offered increasingly exciting possibilities to replace conventional metallic material classes and even surpass them in terms of characteristic values, because of their high mechanical values with comparably low densities at the same time. The aerospace and energy sectors in particular benefit from this, as the use of CMCs allows structures exposed to high thermal loads to be lighter, more durable or with improved efficiency [5]. Classic representatives of CMCs are primarily carbon-carbon (C/C), carbon fibre reinforced silicon carbide (C/SiC) and silicon carbide fibre reinforced silicon carbide (SiC/SiC). However, the disadvantage of all these materials is their use at elevated temperatures under atmospheric conditions. The erosion and oxidation of carbon-based materials already starts at around  $400 \text{ }^\circ\text{C}$ , SiC/SiC materials on the other hand lose their application possibilities from about  $1600 \text{ }^\circ\text{C}$  due to active oxidation of the silicon containing phases [6–8]. This disqualifies these materials, without complex active cooling, for certain applications in re-entry bodies, wing leading edges, scramjet and ramjet engines and generally structures in hypersonics where operating temperatures of over  $1700 \text{ }^\circ\text{C}$  can be reached [2, 9]. Instead, the group of Ultra-High Temperature Ceramics (UHTCs) can be used. These are usually chemical binary compounds (borides, nitrides, carbides and oxides) of refractory metals, which are known for their high melting temperatures, usually far above  $3000 \text{ }^\circ\text{C}$ , their operating temperatures above  $2000 \text{ }^\circ\text{C}$ , as well as their resistance to erosion and oxidation. Examples for UHTCs are zirconium diboride (ZrB<sub>2</sub>), zirconium carbide (ZrC), hafnium diboride (HfB<sub>2</sub>) or titanium diboride [10, 11]. However, since these ceramics behave intrinsically brittle, the embedding of carbon or ceramic fibres in a UHTC matrix achieves damage tolerance and thus a wide range of applications under high thermal and mechanical loads. This group of materials is called Ultra-High Temperature Ceramic Matrix Composites (UHTCMCs). Notable representatives are carbon fibre reinforced zirconium diboride (C/ZrB<sub>2</sub>) and carbon fibre reinforced hafnium diboride (C/HfB<sub>2</sub>) [12, 13]. At the German Aerospace Center (DLR), a UHTCMC material based on carbon fibres and a zirconium diboride matrix is being developed utilizing a Reactive Melt Infiltration (RMI) process. This RMI process comprises three stages: preform fabrication, pyrolysis, and the actual melt infiltration. The process can be seen in Fig. 1.

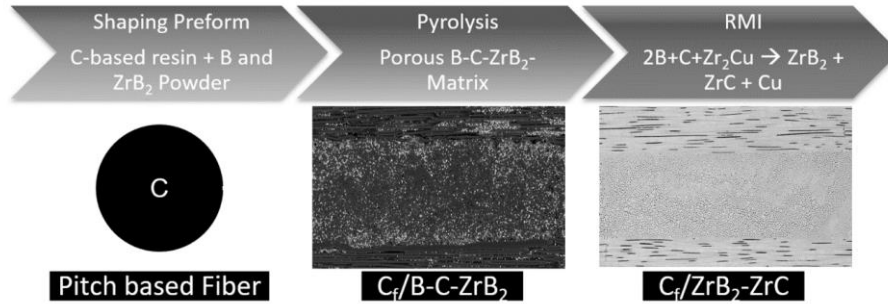
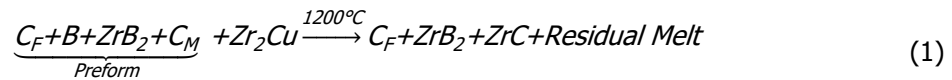


**Fig 1.** RMI process route for the production of UHTCMCs, with images of the microstructure after pyrolysis and after RMI

The foundation for the material properties of the final ceramic, including the matrix composition, is established in the initial preform production, which therefore is a crucial step in the process. A boron- and zirconium diboride-based slurry is infiltrated into pitched-based carbon fibre fabric. The boron powder serves here as a reaction source for the subsequent infiltration with the zirconium melt, whereas the  $ZrB_2$  serves as a supporting grain and is intended to partially absorb the exothermic reaction heat as an inert reaction participant. Subsequently of the powder infiltration, the preforms are consolidated with the assistance of a carbonaceous precursor, pyrolysed, and infiltrated with molten  $Zr_2Cu$  to obtain the UHTC matrix by in situ reaction with the preform elements. During pyrolysis, all volatile components of the preform are split off and a pore system forms within the matrix. During melt infiltration, the liquid zirconium-alloy melt infiltrates into this fine pore system due to the capillary forces and reacts with the preform elements in situ to form  $ZrB_2$  and  $ZrC$  according to Eq. 1. A zirconium copper alloy is used to lower the melting point to allow infiltration at  $1200\text{ }^\circ\text{C}$  to minimize degradation of the carbon fibres which occurs increasingly at higher temperatures.



The advantages of this process are a near-net-shape production and short process times with inexpensive raw materials. Moreover this process enables an embedding of the fibres into the component according to the actual load paths [14, 15]. At the current state of research, the most significant drawback is the relatively high proportion of unreacted residual melt within the UHTCMC matrix, as well as the still occurring degradation of fibre edge regions due to the highly reactive zirconium melt. For this reason, the current manufacturing process was further developed to increase the UHTC ratio of the matrix while reducing the amount of unreacted alloy at the same time, and to understand property changes in the material under high temperature conditions. For this purpose, mechanical behavior was investigated under room temperature and at elevated temperature conditions at  $900\text{ }^\circ\text{C}$ .

## 2. Methods and raw materials

As reinforcement material for the UHTCMC production the pitch-based carbon fibre GRANOC XN-80-60S (Nippon Graphite Fibre Corporation, Japan) with a fibre diameter of  $10\mu\text{m}$  was used. A unidirectional fabric and a plain weave fabric are available for this fibre. In this study the unidirectional fabrics were used. In the current production of UHTCMCs using RMI, the carbon fibre fabric is first infiltrated with a water-based slurry using a foulard. The slurry has a solids content of 50 wt%, which is made up of boron powder (25 wt%) and  $ZrB_2$  powder (75 wt%). The amorphous boron powder for the slurry was supplied by Bayern Chemie GmbH (Germany). Zirconium diboride powder was provided by Höganäs (Sweden). A Partica LA-960 Laser Scattering Particle Size Distribution Analyzer (HORIBA Europe GmbH, Germany) was used to determine the particle sizes. A foulard from Mathis AG (Switzerland) was used to infiltrate the slurry into the fabric layers. The principle of a foulard consists of two counter-rotating rollers that apply pressure to each other. A slurry bath wets the fabric and the physical force of the rollers infiltrates the slurry into the fabric. This principle can be seen in Fig. 2 on the left. In the state-of-the-art process, both powders are used as supplied and are not treated. However, it was found, that slurry infiltration via foulard leads to inhomogeneous particle distribution

throughout the preform, as can be seen in Fig. 2 on the right side. Here the  $ZrB_2$  particles can be seen as white spots whereas boron powder can't be seen due to the color contrasts, but as the particle size of the boron powder is equal or smaller than the  $ZrB_2$  it can be assumed that the boron particles infiltrate slightly better into the fabrics. For the adapted process the powders were ball-milled in isopropyl alcohol using a Pulverisette 6 planetary ball mill (Fritsch GmbH, Germany) before further processing into the slurry.

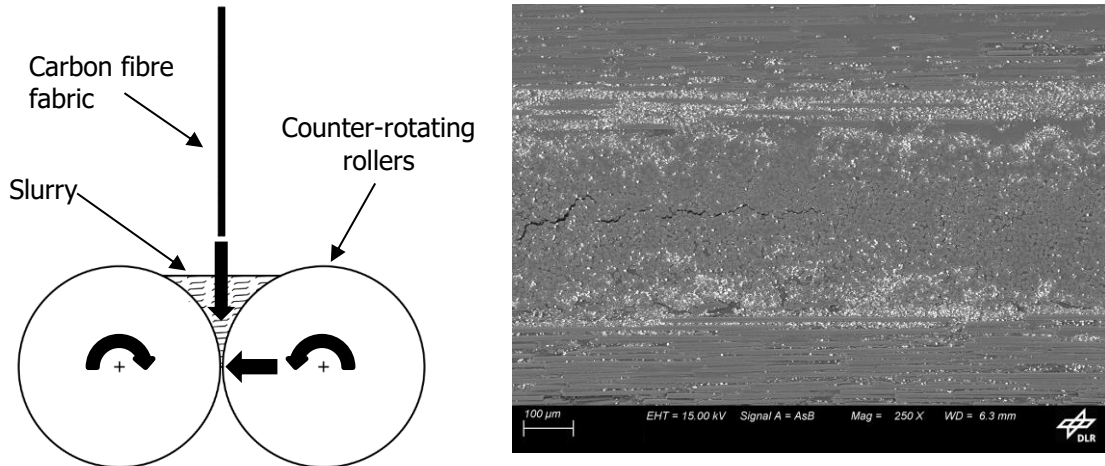


**Fig 2.** principle of slurry infiltration using a foulard (left); inhomogeneous particle distribution in the fibre rovings with initial slurry after infiltration – in white  $ZrB_2$  powder (SEM picture 250x; right)

After infiltration, the fabric layers are dried, stacked and consolidated with the addition of a carbon-based precursor. A laboratory furnace from Diekmann GmbH (Germany) was used for the subsequent high-temperature steps of pyrolysis and melt infiltration process. The samples were then pyrolyzed at temperatures over 1200 °C to reduce the preform matrix to pure carbon, boron and  $ZrB_2$ . Finally, the preforms were melt infiltrated at 1200 °C for 3 minutes. For this purpose, the oven was equipped with a height-adjustable lifting device. For melt infiltration, the eutectic zirconium-copper alloy  $Zr_2Cu$  (HMW Hauner GmbH & Co. Kg) was selected. Copper was chosen as an alloying element to lower the melting temperature (pure Zr 1855 °C;  $Zr_2Cu$  1002 °C) and hence minimize fibre degradation at melt infiltration. Microstructural analysis was performed using scanning electron microscopy (SEM) and energy dispersive X-ray spectroscopy (EDX). A Zeiss GeminiSEM Ultra plus (Carl Zeiss AG, Germany) with a X-Max EDX Detector from Oxford Instruments (United Kingdom) was used for this purpose. All SEM pictures were taken using the angle selective backscattered detector. ImageJ (Version 1.54f) was used to analyze the microstructures in terms of elemental composition and UHTC contents. Mechanical evaluation of the UHTCMCs was conducted via 3-point bending tests at both room temperature and at elevated temperature based on the norm DIN EN 658-3. For room temperature tests a universal testing machine Zwick 1494 (ZwickRoell AG, Germany) was used. The DLR in-house Indutherm test machine was selected for the high-temperature tests, which was operated under vacuum (pressure < 1 mbar) to provide protection for the machine. Both machines were operated at a controlled crosshead speed of 1 mm/min and a support span of 50 mm. The bending strength was calculated from the maximum loads. Sample geometry for both test series was fixed at 60 x 10 x 2.5 mm<sup>3</sup>. Room temperature samples were equipped with strain gauges to measure additional values. Microscope images were taken with a Keyence VHX-S550E digital microscope (Keyence, Japan) to evaluate the fracture behavior of the UHTCMC samples at room temperature and at elevated temperature. Density and porosity were determined according to the Archimedes method (DIN EN 993-1).

### 3. RMI Development and Mechanical Testing

#### 3.1. RMI Development

This current RMI process is to be further developed with a focus on improving the matrix composition and lowering the residual melt phases. In this regard, particular attention is given to the initial slurry infiltration process in which the boron and  $ZrB_2$  powders are infiltrated into the pitch-based carbon fibre fabrics. The goal is to achieve homogeneous infiltration with a high powder deposition into the fabrics

down to the carbon fibre rovings, as Fig. 2 showed the currently inhomogeneous slurry infiltration into the carbon fabrics. To achieve a higher infiltration quality, either the slurry has to be improved or a new infiltration process can be developed, or a combination of both. The first step here is to adapt the slurry before adapting the process in a second step. The new slurry infiltration method investigated, focuses on improving particle distribution and particle size to increase the UHTC matrix proportion throughout the composite and especially in the fibre bundles itself. As a first approach, the influence of the particle size of boron and  $ZrB_2$  was investigated. First, the particle sizes of the as received powder were measured. The amorphous boron powder had a  $d_{50}$  value (median particle size) of  $2.03 \mu m$  and the zirconium diboride powder had a  $d_{50}$  value of  $2.87 \mu m$ . Afterwards the maximum particle size with which infiltration into the fibre bundles is possible was determined. This maximum required particle size can be determined via the cavity size of the packing density of the fibres. A round cross-section can be assumed for carbon fibres. For the densest packing of a fibre bundle, the densest circular packing with a maximum packing density of 0.907 can also be used for the most conservative approach. In conjunction with a fibre diameter of  $10 \mu m$ , this results in a maximum particle size of  $1.54 \mu m$ . As particles normally have an approximately normal distribution, the applied  $d_{50}$  value should be below  $1 \mu m$ . Based on this the powders were ball milled up to 90 minutes in isopropyl alcohol. Isopropyl Alcohol was used to prevent unwanted reactions that could lead to the formation of hydrogen. The resulting median particle sizes were  $d_{50} = 0.33 \mu m$  for boron and  $d_{50} = 0.59 \mu m$  for  $ZrB_2$ . Fig. 3 shows the measured particle size distributions for boron and zirconium diboride powder as received and after ball milling. The relative distribution  $q$  [%] (shown in black) and the cumulative distribution  $Q$  [%] (shown in red) of the powders are plotted against the particle size in a logarithmic diagram. This clearly shows how milling appears to have an influence on coarse and fine particles, as the curves generally shift to the left towards finer particle sizes after milling. Both the maximum particle sizes and the smallest particle sizes decrease. The unground particles also appear to be partially agglomerated, which are measured here as particles larger than  $10 \mu m$ .

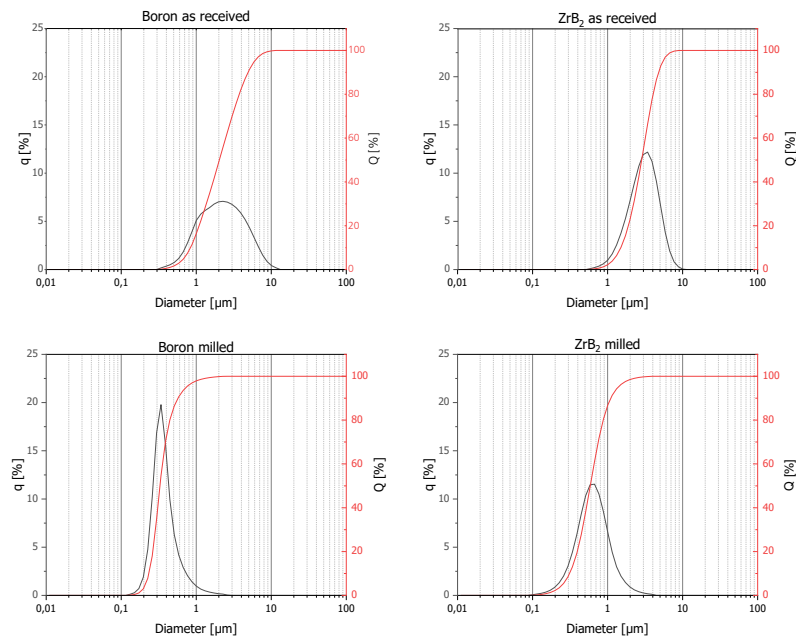


**Fig 3.** Particle size distributions for boron and  $ZrB_2$  as received and milled

In order to investigate the influence on of the milled powders on the infiltration, carbon fibre fabrics were infiltrated with a  $ZrB_2$  only slurry by a vacuum assisted process and analyzed by means of SEM. Fig. 4 shows the resulting SEM images (500x) with the received powder on the left and the ground powder on the right. It can be clearly seen that the ground powder infiltrates much better into the fibre bundle and leads to a significant increase in quantity and homogeneity. As the ground boron powder is even finer than the  $ZrB_2$ , it can be assumed that this effect is even more noticeable with the milled boron. The ground boron and  $ZrB_2$  particles were then used to produce a comparable slurry to the non-ground powder slurries, followed by fabric infiltration by foulard, drying and processing to UHTCMCs



by melt infiltration. UHTCMCs manufactured according to the state-of-the-art process are hereinafter referred to as Reference UHTCMC material and samples with the milled powders as improved UHTCMC material.

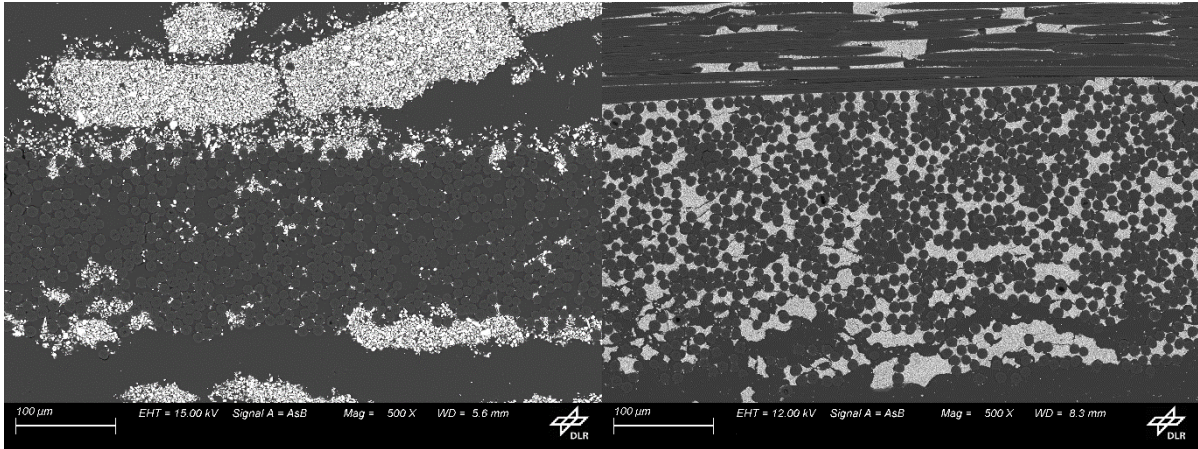


**Fig 4.** Infiltration test with  $ZrB_2$  only slurry with particles as received (left) and ground up (right); (SEM pictures 500x)

### 3.2. Microstructural Analysis

SEM and EDX enable examination of the microstructural features, including the arrangement and dispersion of zirconium diboride and zirconium carbide within the matrix. Zirconium carbide is mainly formed around the fibers due to the reaction between fibre and melt in melt infiltration. Fig. 5 shows the microstructures for the reference material with as received powders on the left, as well as for the improved slurry material with ground powders on the right, both at a magnification of 3000x. In these pictures Carbon fibres are shown in black, zirconium diboride in dark grey, zirconium carbide in grey and remaining melt in light grey. The percentages of elemental composition for both UHTCMCs is shown in Table 1 each rounded to one decimal place. To compare the elemental compositions of the matrices the Matrix-only compositions of the Composites were calculated and are shown in Table 2. A comparison of these two UHTCMCs shows directly that grinding the particles makes the  $ZrB_2$  phases significantly smaller. However, this also means that the zirconium diboride is much more homogeneously distributed within the matrix as can be clearly seen in Fig. 5. In comparison, the sample without ground powder shows larger areas in which the matrix consists only of residual melt without or with only a low UHTC content as can be seen in the SEM picture as well. In addition, grinding the base powders increases the overall UHTC content of the matrix from 61.1% to 71.1% due to this improved infiltrability, which means an increase of 16.4%. At the same time, this congruently reduces the amount of low-melting Zr-Cu residual phases in the matrix from 38.9% to 28.9%.

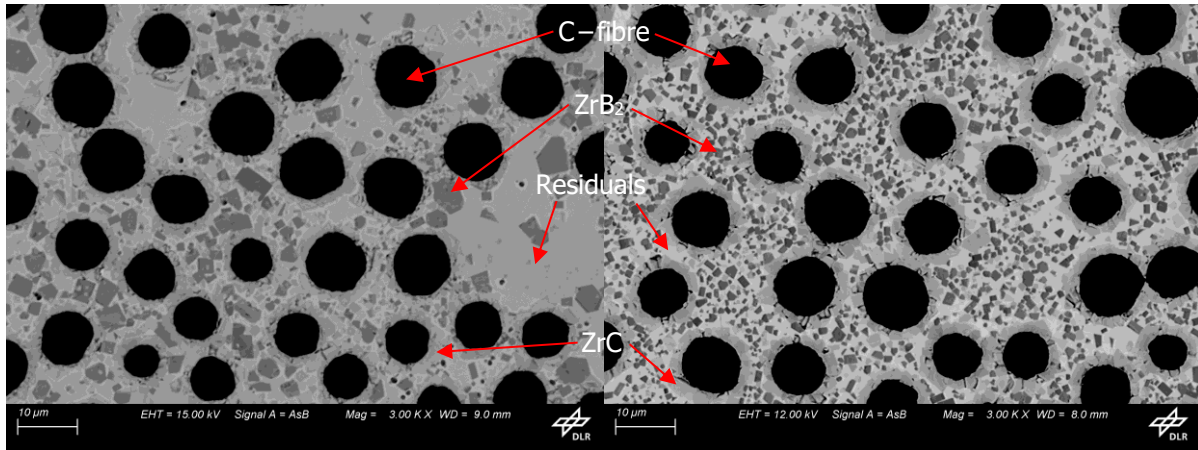


**Fig 5.** Microstructure of reference UHTCMC material (left) and improved UHTCMC Material (right); (SEM pictures 3000x)

**Table 1** Elemental Composition of the UHTCMCs

	<b>C–fibre</b>	<b>UHTCs</b>	<b>Residuals</b>
<b>Reference UHTCMC Material</b>	28.0%	44.0%	28.0%
<b>Improved UHTCMC Material</b>	26.0%	52.6%	21.4%

**Table 2** Matrix-only Composition of the UHTCMCs

	<b>UHTCs</b>	<b>Residuals</b>
<b>Reference Material</b>	61.1%	38.9%
<b>Ground Powder Material</b>	71.1%	28.9%

Energy-dispersive X-ray spectroscopy was used to analyze the elemental composition of the samples more precisely. In particular, the remaining copper content within the UHTCMCs was determined using EDX. Fig. 6 shows the EDX distribution images for the elements zirconium, carbon and copper for an SEM image with 1000x magnification as well as the respective element distribution sum spectra for the reference sample on the left and the adapted sample on the right, with values given in atomic percent. Boron is not recognized by the detector, as the boron peak is overlaid by the clearly pronounced carbon peak. For the reference UHTCMC, the remaining copper content is 3.1 at%, whereas in the improved sample only 1.4 at% copper is present due to the increase in the ceramic phases, which reduces the residual melt content. This represents a decrease of 55%. Because of the low melting point of copper (1085 °C), minimizing the copper quantity inside of the composite helps to increase the high-temperature properties of the ceramic. It can therefore be seen that grinding the source powders improves the homogeneity of the UHTC matrix and increases the overall UHTC content of the matrix while lowering the residual copper content. Although the copper content could be reduced, copper still remains in the sample.

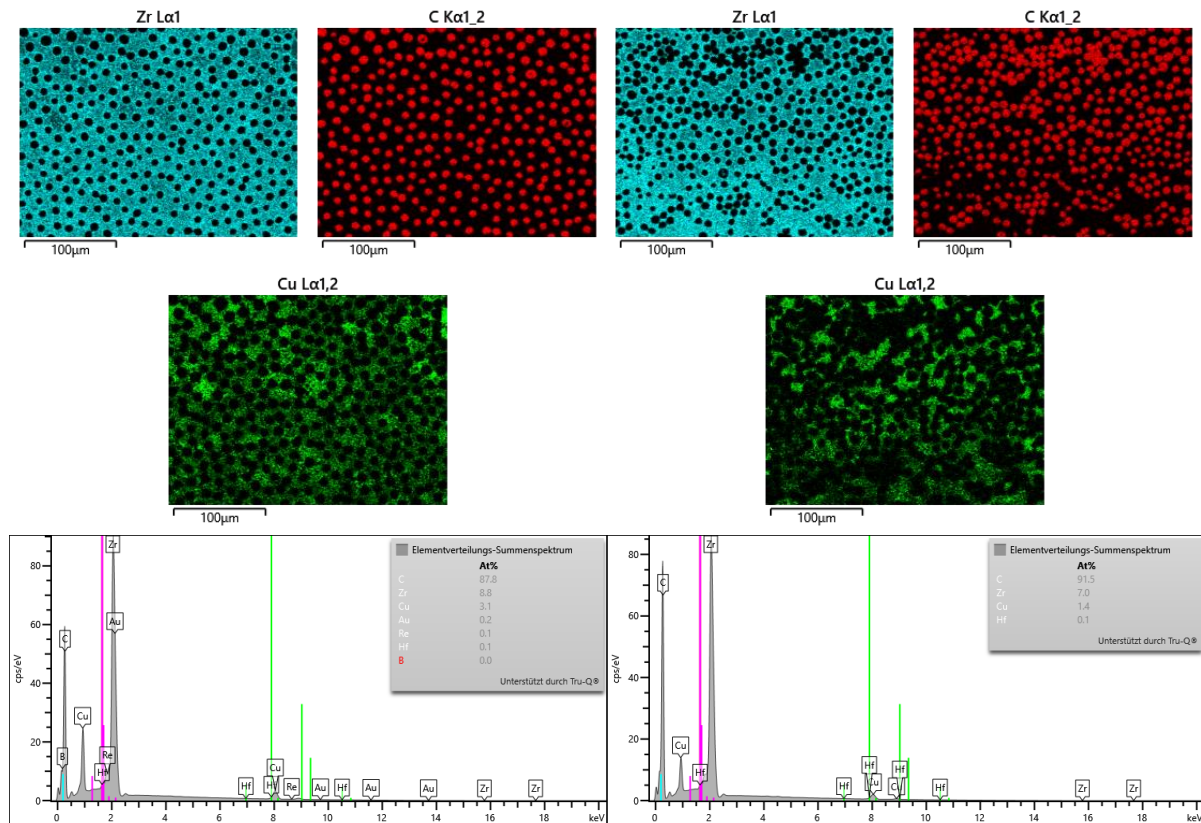


**Fig 6.** EDX distribution images for zirconium, carbon and copper and EDX sum spectra for the reference sample (left) and improved sample (right)

### 3.3. Mechanical Testing

Finally, bending tests were performed on UHTCMC samples with an improved matrix to determine some of the mechanical properties. The tests were carried out at room temperature (25 °C) and at an elevated temperature of 900 °C. Table 3 shows the mechanical properties generated by 3-point bending at room temperature with the corresponding standard deviations. A mean bending strength of 312.90 MPa could be reached at an elongation at break of 0.38% with a young's modulus of 129.53 GPa. At 900 °C, on the other hand, an average bending strength of 190.19 MPa with a standard deviation of 35.08 MPa was reached. This corresponds to 60.78% of the bending strength at room temperature. For a better visualization of these values and a good estimation of the distribution of the individual measured values, Fig. 7 shows the boxplots for the 3-point bending at 900 °C and room temperature. The green line shows the median value of the bending strengths. The lower blue line is named the lower quartile, as the upper one is named the upper quartile. Between these two values, in the box, 50% of the measured values are distributed. For the whiskers, the upper and lower ends of the lines outside the boxes, the highest and lowest measured values were used here. The overall decrease in strength with increasing temperature can be explained primarily by the softening of the Zr-Cu residual phases, that were clearly visible in Fig 6. The corresponding binary phase diagram of this system shows the first melting phases already from a temperature of 920 °C. A further reduction in the residual phases should therefore be able to further increase the high-temperature strengths. In addition, increasing the fibre volume content (currently quite low < 30%, compare Table 1) should increase the general strength over the entire temperature range.



**Table 3** Mechanical values of improved UHTCMC at room temperature (25 °C)

	<b>Bending Strength</b>	<b>Young's Modulus</b>	<b>Elongation at Break</b>
<b>Mean Value</b>	312.90 MPa	129.53 GPa	0.38%
<b>Standard Deviation</b>	55.22 MPa	9.38 GPa	0.10%

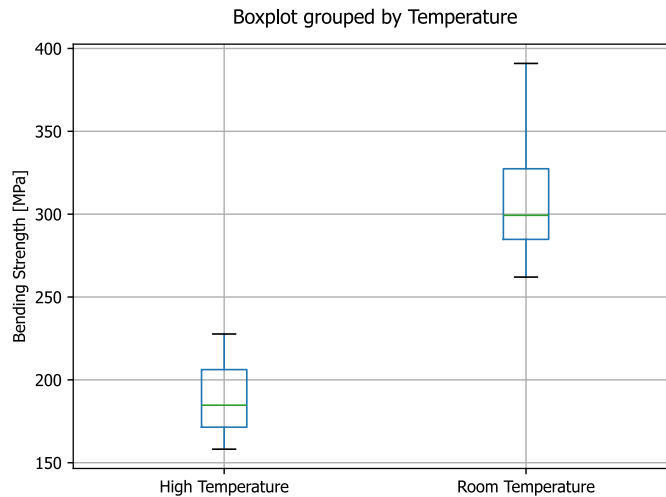


**Fig 7.** Boxplots of the results of the 3-point bending test for room temperature and 900 °C

Fig. 8 shows examples of two 3-point bending specimens in cross-section after testing at 25 °C (left) and 900 °C (right) at a magnification of 100x. The matrix cracks caused by the tests can be clearly recognized in both samples. These images clearly show that, in contrast to a typical fracture of a monolithic ceramic, there is no brittle fracture behavior at either room temperature or at 900 °C. Instead, the crack deflection effect can be observed: the crack does not run straight through the specimen once being initiated but is repeatedly deflected at fibre bundles. Furthermore, none of the samples showed a complete fracture, and thus a catastrophic failure, which indicates a certain damage tolerance of the material both at room temperature and at 900 °C, which is typical for a ceramic matrix composite. However, both cross-sections show pores, as can be seen in Fig. 8. These pores are caused by insufficient infiltration with zirconium melt and reduce the mechanical properties as failure often starts to develop at these defects. It can also be seen that the resulting cracks were probably initiated in the area of pores. By reducing the porosity in the future, it should be possible to further increase the mechanical properties accordingly. With reference to this, Table 4 shows the values for density and porosity for the 3-point bending samples as well as the corresponding standard deviations. The density is 5.27 g/cm<sup>3</sup>. Due to the light carbon fibres (density 2.17 g/cm<sup>3</sup>), this material is therefore lighter than the relevant matrix elements ZrB<sub>2</sub> (6.08 g/cm<sup>3</sup>), ZrC (6.73 g/cm<sup>3</sup>) and Zr-Cu (6.5-8.96 g/cm<sup>3</sup>). The porosity of 6.07% is a relatively high value for ceramics produced by reactive melting processes, where low porosities of less than 5% can normally be achieved. One reason for this is certainly the unidirectional fabric, which has a stabilizing weft fibre made of a polymer that burns out during pyrolysis and leaves behind pores that cannot be filled with the melt by capillary forces. In future, a different type of weave could be used to minimize the formation of this porosity

**Table 4** Density and Porosity of the UHTCMCs

	<b>Density</b>	<b>Porosity</b>
<b>Mean Value</b>	5.27 g/cm <sup>3</sup>	6.07%
<b>Standard Deviation</b>	0.26 g/cm <sup>3</sup>	2.17%

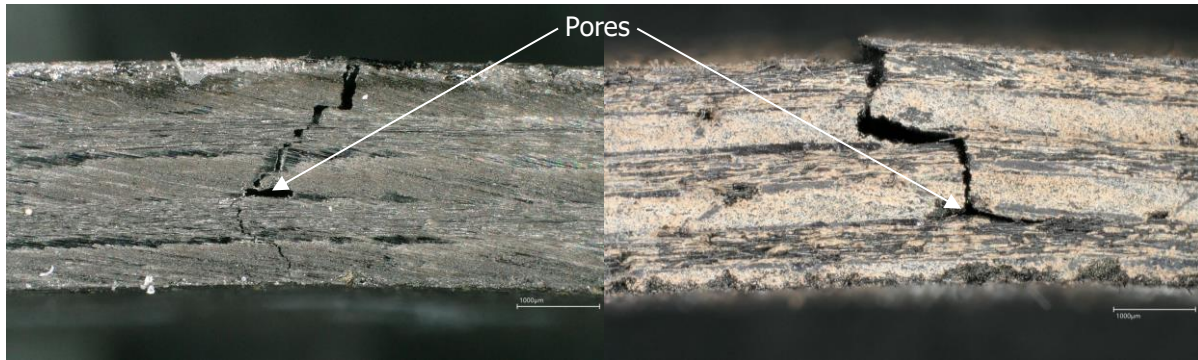


**Fig 8.** Cross-sections of 3-point bending specimens after testing at 25 °C (left) and 900 °C (right) at 100x

#### 4. Conclusion

Due to their material characteristics, the class of UHTCMCs offers the potential for use in hypersonic vehicles, for structural components exposed to high thermomechanical loads. Zirconium diboride-based materials are particularly interesting due to their high temperature stability. DLR is therefore developing a carbon fibre-reinforced ZrB<sub>2</sub>.

It has been demonstrated that Ultra-High Temperature Ceramic Matrix Composites based on zirconium diboride and zirconium carbide can be produced by means of reactive melt infiltration process and, that by adapting the used slurry at the preform production process, an improved particle infiltration could be achieved. This led to an overall increase of the UHTC content by 16,4% and a better, more homogeneous distribution inside of the composite matrix, especially with regard to zirconium diboride. At the same time, the proportion of low-melting copper was reduced by almost 55% to 1.4at%. Low-melting copper phases are a major cause of temperature limitation and should therefore be minimized.

Three-point bending tests at room temperature achieved an average bending strength of 312.90 MPa with an elongation at break of 0.38%. At 900 °C, the flexural strength decreased by 40% to an average of 190.19 MPa. Both at room temperature and at elevated temperature, the UHTCMCs showed typical damage-resistant behavior. This test at 900 °C was intended to generate initial data on this material in order to better understand its behavior at this temperature. By further reducing the amount of copper, or by using a completely new alloy in the future, the high-temperature stability should be further investigated and increased.

#### References

1. Millar, K., Brannon, K.: The rise of hypersonics : Hypersonic weapons and flight breaking new barriers. <https://www2.deloitte.com/us/en/pages/energy-and-resources/articles/rise-of-hypersonics.html> – Accessed 03. January 2024
2. Glass, D.: Ceramic Matrix Composite (CMC) Thermal Protection Systems (TPS) and Hot Structures for Hypersonic Vehicles. In: 15th AIAA International Space Planes and Hypersonic Systems and Technologies Conference : American Institute of Aeronautics and Astronautics, 2008 (International Space Planes and Hypersonic Systems and Technologies Conferences).
3. Sziroczak, D., Smith, H.: A review of design issues specific to hypersonic flight vehicles. In: Progress in Aerospace Sciences 84 (2016), S. 1–28
4. Wright, D., Tracy, C.: The Physics and Hype of Hypersonic Weapons : These novel missiles cannot live up to the grand promises made on their behalf, aerodynamics shows. In: Scientific American (2021), Nr. 325, S. 64–71
5. Roth, R., Clark, J.P. ; Field, F.R.: The potential for CMCs to replace superalloys in engine exhaust ducts. In: JOM - Journal of the Minerals, Metals and Materials Society 46 (1994), Nr. 1, S. 32–35
6. Hülsenberg, D.: Keramik : Springer Vieweg, Berlin, Heidelberg, 2014

7. Jacobson, N., Opila, E., Fox, D., Smialek, J.: Oxidation and Corrosion of Silicon-Based Ceramics and Composites. In: Materials Science Forum - MATER SCI FORUM 251-254 (1997), S. 817–832
8. Gee, S.M., Little, J.A.: Oxidation behaviour and protection of carbon/carbon composites. In: Journal of Materials Science 26 (1991), Nr. 4, S. 1093–1100
9. Justin, J.F., Julian-Jankowiak, A., Guérineau, V., Mathivet, V., Debarre, A.: Ultra-high temperature ceramics developments for hypersonic applications. In: CEAS Aeronautical Journal 11 (2020), Nr. 3, S. 651–664
10. Ionescu, E., Bernard, S., Lucas, R., Kroll, P., Ushakov, S., Navrotsky, A., Riedel, R.: Polymer-Derived Ultra-High Temperature Ceramics (UHTCs) and Related Materials. In: Advanced Engineering Materials 21 (2019), Nr. 8, S. 1900269
11. Wuchina, E., Opila, E., Opeka, M., Fahrenholtz, B., Talmy, I.: UHTCs: Ultra-High Temperature Ceramic Materials for Extreme Environment Applications. In: The Electrochemical Society Interface 16 (2007), Nr. 4, S. 30–36
12. Paul, A., Jayaseelan, D.D., Venugopal, S., Zapata-Solvas, E., Binner, J. G.P., Vaidhyanathan, B., Heaton, A., Brown, P.M., Lee, W.E.: UHTC composites for hypersonic applications (2012)
13. Tang, S., Hu, C.: Design, Preparation and Properties of Carbon Fiber Reinforced Ultra-High Temperature Ceramic Composites for Aerospace Applications: A Review. In: Journal of Materials Science & Technology (2016)
14. Küttemeyer, M.: Development of Ultra High Temperature Matrix Composites using a Reactive Melt Infiltration Process. Karlsruher Institut für Technologie (KIT). Ph.D. thesis. 2021
15. Rubio, V., Ramanujam, P., Binner, J.: Ultra-high temperature ceramic composite. In: Advances in Applied Ceramics 117 (2018), s56-s61